

---

# 6-[Fluorine-18]Fluorodopamine Pharmacokinetics and Dosimetry in Humans

David S. Goldstein, Lisa Coronado and Irwin J. Kopin

*Clinical Neuroscience Branch, National Institute of Neurological Disorders and Stroke and Radiation Safety Branch,  
Division of Safety, Office of the Director, National Institutes of Health, Bethesda, Maryland*

---

PET scanning after injection of 6-[<sup>18</sup>F]fluorodopamine visualizes tissue sympathetic innervation. Organ dosimetric estimates for 6-[<sup>18</sup>F]fluorodopamine have relied on studies of rats and dogs and on literature about the fate of other radiolabeled catecholamines. This report uses empirical clinical findings in healthy volunteers to refine and extend these estimates. **Methods:** Thoracic PET scanning was conducted and arterial blood and urine samples were obtained after intravenous injection of 6-[<sup>18</sup>F]fluorodopamine into 10 normal volunteers. **Results:** The main target organs for 6-[<sup>18</sup>F]fluorodopamine-derived radioactivity were the wall of the urinary bladder (3.3 rem for a 4-mCi dose and 3.31-hr voiding interval) and the kidneys (2.9 rem for a 4-mCi dose) due to urinary excretion of radioactive metabolites of [<sup>18</sup>F]-6F-DA. The estimates were about one-fourth those predicted from studies of laboratory animals. **Conclusions:** At administered doses required to visualize the left ventricular myocardium in humans, a 6-[<sup>18</sup>F]fluorodopamine injection produces acceptable absorbed radiation doses, with the highest doses to the urinary collecting system.

**Key Words:** 6-[fluorine-18]fluorodopamine; sympathetic innervation; dosimetry; norepinephrine

**J Nucl Med 1994; 35:964–973**

---

**P**ET scanning after systemic administration of 6-[<sup>18</sup>F]fluorodopamine ([<sup>18</sup>F]-6F-DA) provides a new means for visualizing tissue sympathetic innervation, especially in the heart. Studies of rats, dogs and humans have shown that the fate of injected [<sup>18</sup>F]-6F-DA resembles that of injected radiolabeled DA (1–7), because sympathetic nerves avidly remove [<sup>18</sup>F]-6F-DA. After intraneuronal translocation of [<sup>18</sup>F]-6F-DA into vesicles containing dopamine- $\beta$ -hydroxylase, [<sup>18</sup>F]-6F-DA is converted to [<sup>18</sup>F]-6F-norepinephrine ([<sup>18</sup>F]-6F-NE), a fluorinated analog of the sympathetic neurotransmitter. Fluorine-18-6F-DA is a substrate for both monoamine oxidase and catechol-O-methyltransferase, forming [<sup>18</sup>F]-6F-dihydroxyphenylacetic acid and [<sup>18</sup>F]-6F-homovanillic acid, fluorinated analogs of metabolites of DA; and 6F-NE appears to be released and

metabolized similarly to [<sup>3</sup>H]NE during sympathetic stimulation.

Previous dosimetric estimates after [<sup>18</sup>F]-6F-DA injection relied on studies of rats and dogs and on literature about the disposition of other injected radiolabeled catecholamines (8). This report refines and extends these estimates based on PET and neurochemical findings after injection of [<sup>18</sup>F]-6F-DA into healthy humans.

Fluorine-18-6F-DA PET scanning can visualize sympathetic innervation but cannot distinguish tissue radioactivity due to [<sup>18</sup>F]-6F-DA from radioactivity due to [<sup>18</sup>F]-6F-NE and from metabolites of [<sup>18</sup>F]-6F-DA and of [<sup>18</sup>F]-6F-NE; and the validity of analyses of curves relating tissue radioactivity to time (time-activity curves) for examining regional sympathoneural outflow has not yet been established (9). Assessments of the kinetics of [<sup>3</sup>H]-L-NE and its metabolites in a vascular bed can provide comprehensive information about aspects of sympathoneural function, such as neuronal uptake and intraneuronal metabolism (10–12), but cannot detect heterogeneity of innervation or regional differences in catecholamine disposition within an organ. Combined assessments by [<sup>18</sup>F]-6F-DA PET scanning and [<sup>3</sup>H]-L-NE kinetics therefore have the potential to provide complementary information about sympathetic innervation and function. In order to predict organ radiation doses after administration of both radioactive compounds into the same human subjects, the present study presumed the generally similar fate of [<sup>18</sup>F]-6F-DA with that of other radiolabeled catecholamines and applied the empirical [<sup>18</sup>F]-6F-DA PET scanning data to estimate organ radiation doses after injection of [<sup>3</sup>H]-L-NE.

## MATERIALS AND METHODS

### Subjects and Experimental Sequence

PET studies were conducted in 10 healthy male volunteers (age 24–69 yr, weight 70–100 kg, mean weight 79.0 kg) who gave informed consent. Screening medical history, physical examination, electrocardiogram and blood and urine tests were normal. The study protocol was approved by the Institute Clinical Research Subpanels of the NINDS and NHLBI, the NIH PET Scientific Review Committee and the NIH Radiation Safety Committee; and [<sup>18</sup>F]-6F-DA was administered to humans under Investigational New Drug Application 33,866.

The subjects were studied after having fasted overnight and having refrained from cigarette smoking, caffeinated or decaffeinated

---

Received Oct. 13, 1993; revision accepted Mar. 14, 1994.  
For correspondence or reprints contact: Dr. David S. Goldstein, NINDS, NIH, Building 10 Room 5N262, Bethesda, MD 20892.

ated coffee and alcohol for at least 12 hr. The subjects were allowed to eat a light breakfast (such as toast and orange juice or cereal and skim milk) before arriving at the PET area of the NIH Clinical Center at about 10:30 AM.

An antecubital venous catheter was inserted for administration of [ $^{18}\text{F}$ ]-6F-DA. The subject was positioned in a Posicam body scanner (Positron Corporation, Houston, TX) with the subject's thorax in the gantry. The Posicam body scanner produces 21 overlapping planes (12.5 mm thickness, 5.1 mm apart, pixel volume 1.7 mm<sup>3</sup>, transverse spatial resolution 6.8 mm). A transmission scan using a rotating pin source was obtained to confirm the location of the heart before administration of [ $^{18}\text{F}$ ]-6F-DA and to correct the emission scans for photon attenuation.

For continuous monitoring of blood pressure and for drawing blood samples, a brachial or radial artery catheter was inserted percutaneously after anesthesia of the overlying skin using lidocaine. The catheter was flushed occasionally with a dilute heparin solution.

Fluorine-18-6F-DA was synthesized either from 6-[ $^{18}\text{F}$ ]fluorodopa (Ref. 6, 9 subjects) or by a direct method (Ref. 7, 1 subject). The drug passed quality control testing (chemical and radiochemical purity at least 90%, Ref. 13) before being administered. Fluorine-18-6F-DA dissolved in about 10 cc of normal saline was infused by syringe pump at a constant rate over 3.0 min (1.0 min in one subject). The doses were 1 (one study), 1.5 (one study), 2 (one study), 3 (one study) and 4 (six studies) mCi, with a mean dose of 3.21 mCi. The specific activities of the [ $^{18}\text{F}$ ]-6F-DA ranged from 188 to 357 (mean 254) mCi/mmol at the time of injection.

Continuous PET scanning was conducted from the beginning of drug administration until 2.5–3.0 hr later. For purposes of data analysis, scanning intervals ranged from 5 to 30 min. Data acquisition was not gated to the electrocardiogram.

Arterial blood was obtained just before drug administration and at 0.25, 0.50, 0.75, 1.0, 2.0, 3.0, 3.5, 4.0, 5.0, 10, 15, 30, 45, 60, 90, 120, 150, and 180 min after drug administration. The samples at 0.25, 0.50, 0.75, 2.0 and 3.5 min were 1 ml, the baseline sample was 10 ml, and the other samples were 5 ml. The total amount of blood drawn was about 100 ml.

In one subject, a Foley catheter was placed for continuous collection of urine during PET scanning. In all subjects, urine was obtained after scanning ended (mean 3.31 hr after [ $^{18}\text{F}$ ]-6F-DA injection).

Aliquots of whole arterial blood and arterial plasma (obtained after centrifugation at room temperature for 5 min) were assayed directly for concentrations of total radioactivity using a calibrated scintillation well counter. Arterial blood samples for subsequent assays of 6F-compounds after complete radioactive decay were collected in chilled, evacuated, heparinized glass tubes and placed immediately on ice. The plasma was separated by refrigerated centrifugation, transferred to plastic cryotubes and stored at  $-70^{\circ}\text{C}$ . Arterial plasma concentrations of 6F-dopamine and metabolites were assayed by liquid chromatography with electrochemical detection after addition of internal standards (dihydroxybenzylamine or 2-fluorodopamine) and batch alumina extraction (14, 15).

The first void of urine after the PET scanning session was collected in a preweighed urinal and the volume and time were recorded. Three 300- $\mu\text{l}$  aliquots were assayed for radioactivity. Another aliquot was acidified with 6N HCl and stored at  $-70^{\circ}\text{C}$  until assayed for unlabeled fluorinated metabolites of 6F-dopamine and 6F-norepinephrine within about 1 mo.

## Data Analysis

Cardiac PET images were analyzed as described previously (6, 7). Circular regions of interest (ROIs) with diameters about one-half the width of the ventricular wall were created using a time-averaged image for a single slice that depicted the left ventricular free wall, chamber and septum. The radioactivity concentrations for two ROIs each in the left ventricular free wall and septum were averaged. Circular ROIs were also analyzed in areas corresponding to the liver and gallbladder.

To construct time-activity curves, the logs of the mean concentrations of radioactivity (each concentration adjusted for the dose/kg body weight, i.e., expressed in units of nCi-kg/cc-mCi) in tissue and in arterial blood and plasma were expressed as a function of time after tracer injection. Mean values are expressed  $\pm$  s.e.m. The specific activity of [ $^{18}\text{F}$ ]-6F-DA at the time of injection and the assayed plasma concentrations of [ $^{18}\text{F}$ ]-6F-DA were used for estimating the proportions of the total plasma radioactivity resulting from [ $^{18}\text{F}$ ]-6F-DA and its metabolites.

Mono-exponential, bi-exponential and tri-exponential curve fitting was used to describe the empirical relationships between mean radioactivity concentrations (in myocardium, liver, blood and plasma) and time using a "peeling" approach, as follows. The mono-exponential line of best fit (CricketGraph, Cricket Software, Malvern, PA) was determined for the averaged data during the late phase between 60 and 180 min after injection of [ $^{18}\text{F}$ ]-6F-DA. From the y-intercept value and slope, estimated values were obtained for the period between the peak mean concentration after the [ $^{18}\text{F}$ ]-6F-DA injection (at 7.5 min for myocardium and at 3.0 min for blood and plasma) and about 40 min later. The difference between the estimated and empirical values was graphed and the mono-exponential line of best fit for the early phase thereby determined. From the equations for the two lines, bi-exponential curves were generated and compared visually with the empirical data. For myocardial and hepatic radioactivity, bi-exponential curve fitting described the empirical results very well; for blood and plasma, however, a third term (tri-exponential curve of best fit) was required, for the period between 10 and 45 min after initiation of the [ $^{18}\text{F}$ ]-6F-DA injection, and the mono-exponential line of best fit for this period was determined as described above.

Integrated radioactivity exposures in the wall of the urinary bladder, kidneys, portal-drained viscera, liver, heart, gallbladder, brain and other organs were calculated using equations described previously (7) or derived in the Discussion.

Estimates of absorbed radiation doses to body organs were calculated by multiplying the integrated radioactivity exposures by S-factors (MIRDOSE program, IBM PC Version—Jan, 1988, Oak Ridge Institute for Science and Education, Oak Ridge, TN), which relate cumulated activity ( $\bar{A}$ , in  $\mu\text{Ci}\cdot\text{hr}$ ) to absorbed dose.

The MIRDOSE program provides absorbed dose estimates based on calculations of organ "residence time",  $\tau$ , defined as the quotient obtained by dividing  $\bar{A}$  by the injected activity ( $A_0$ , in  $\mu\text{Ci}$ , Ref. 16). The residence time can be viewed as an "average" life of the administered activity in an organ. The version of the MIRDOSE program available to us did not take into account bi- or multi-exponential declines in organ radioactivity, and because radioactivity after [ $^{18}\text{F}$ ]-6F-DA injection declined in at least a bi-exponential manner in all organs assayed, we calculated total absorbed doses by summing values for  $\bar{A} \cdot S$  for target organs using a table of S-factors for  $^{18}\text{F}$  and standard spreadsheet software.

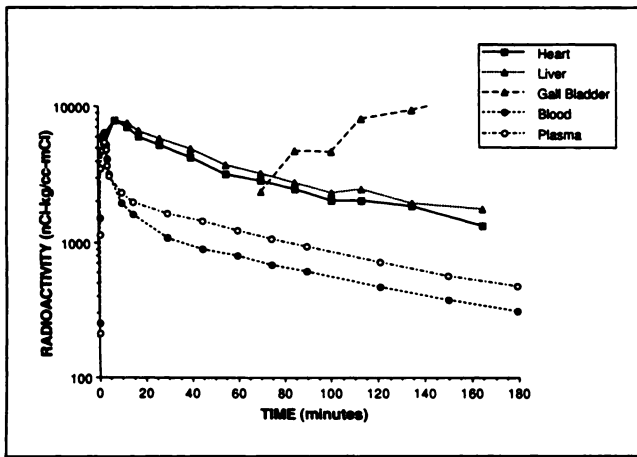


**FIGURE 1.** Mean radioactivity concentrations (adjusted for the dose/kg body weight) in the left ventricular myocardium, liver, gallbladder, blood and plasma after injection of 6- $^{18}\text{F}$ fluorodopamine into humans.

## RESULTS

Thoracic PET scanning after  $^{18}\text{F}$ -6F-DA injection visualized the left ventricular myocardium in all 10 subjects, the liver in 6 subjects and the gallbladder in 2 subjects.

Little or no  $^{18}\text{F}$ -6F-DA-derived radioactivity was noted in regions corresponding to bone, lung parenchyma, skeletal muscle, skin or the adrenal glands, with the exception of radioactivity noted bilaterally in the posterobasal (dependent) portions of the lungs.

Beginning soon after the injection of  $^{18}\text{F}$ -6F-DA, myocardial and hepatic concentrations of  $^{18}\text{F}$ -6F-DA-derived radioactivity exceeded that in arterial blood (Fig. 1, Table 1), due to retention of tissue radioactivity as blood radioactivity rapidly declined. Since during PET scanning the ventricular myocardial concentration of radioactivity decreased substantially from the peak value (Fig. 1), only at the 3- and 4-mCi doses was the myocardium depicted throughout the 3 hr of PET scanning.

The declines in  $^{18}\text{F}$ -6F-DA-derived radioactivity in the myocardium and liver were bi-exponential (Table 2). In contrast with the progressive decline in  $^{18}\text{F}$ -6F-DA-derived radioactivity in the liver,  $^{18}\text{F}$ -6F-DA-derived radioactivity accumulated in an intrahepatic region corresponding to the gallbladder (Fig. 1), with the radioactivity concentration about 11000 nCi/kg/cc-mCi at the end of the PET scanning.

In the subject with an indwelling Foley catheter,  $^{18}\text{F}$ -6F-DA-derived radioactivity was detected in the first urine

**TABLE 1**  
Mean ( $\pm$  s.e.m.) Radioactivity Concentrations (nCi/kg/cc-mCi) After Injection of 6- $^{18}\text{F}$ Fluorodopamine into Healthy Humans

Time (min)	Blood	Plasma	Heart	Liver
0.52	283 $\pm$ 177	213 $\pm$ 151		
0.78	1651 $\pm$ 400	1141 $\pm$ 268		
1.03	4799 $\pm$ 1396	3505 $\pm$ 837		
2.0	5805 $\pm$ 766	4736 $\pm$ 926		
2.5			6109 $\pm$ 7915	4880 $\pm$ 568
3.0	6256 $\pm$ 983	5436 $\pm$ 1094		
3.6	5207 $\pm$ 699	4809 $\pm$ 701		
4.0	4164 $\pm$ 637	3690 $\pm$ 446		
5.0	3218 $\pm$ 486	3108 $\pm$ 475		
7.5			7915 $\pm$ 747	7885 $\pm$ 918
10.0	1949 $\pm$ 263	2329 $\pm$ 227		
12.5			6886 $\pm$ 609	7539 $\pm$ 847
15.0	1607 $\pm$ 270	1971 $\pm$ 176		
17.5			5888 $\pm$ 547	6669 $\pm$ 287
26.6			5118 $\pm$ 343	5808 $\pm$ 370
30.0	1087 $\pm$ 157	1640 $\pm$ 140		
40.6			4055 $\pm$ 339	4863 $\pm$ 354
45.0	901 $\pm$ 136	1441 $\pm$ 124		
55.6			3046 $\pm$ 329	3728 $\pm$ 443
60.0	809 $\pm$ 113	1222 $\pm$ 106		
70.6			2718 $\pm$ 314	3254 $\pm$ 332
75.0	692 $\pm$ 103	1063 $\pm$ 97		
85.6			2603 $\pm$ 318	2769 $\pm$ 384
90.0	615 $\pm$ 90	939 $\pm$ 83		
101			2076 $\pm$ 266	2328 $\pm$ 310
114			1894 $\pm$ 468	2458 $\pm$ 341
121	473 $\pm$ 72	721 $\pm$ 78		
135			1747 $\pm$ 345	1954 $\pm$ 283
150	382 $\pm$ 60	566 $\pm$ 72		
165			1317 $\pm$ 99	1759 $\pm$ 323
180	322 $\pm$ 70	478 $\pm$ 61		

**TABLE 2**  
Zero-Time Intercepts ( $Y_0$ ) and Biological Disappearance Constants ( $K$ ) for Organ Bi-Exponential or Tri-Exponential Curves of Best Fit After Injection of 6-[ $^{18}\text{F}$ ]Fluorodopamine

Organ	$Y_{0_1}$	$K_1$	$Y_{0_2}$	$K_2$	$Y_{0_3}$	$K_3$
Blood	21921	0.485	1921	0.0988	1249	0.00792
Plasma	18355	0.543	581	0.0447	1933	0.00798
Myocardium	4754	0.0467	4669	0.00739		
Liver	4398	0.0339	4802	0.00633		

$Y_0$  units = nCi·kg/cc·mCi;  $K$  units =  $\text{min}^{-1}$ . Each value derived from best-fit curves applied to mean values in Table 1.

sample, obtained 8 min after the initiation of the injection of [ $^{18}\text{F}$ ]-6F-DA. In this subject, after administration of 2.0 mCi of [ $^{18}\text{F}$ ]-6F-DA, the total amount of radioactivity (corrected for decay) in urine during the first 3 hr was 0.481 mCi, with 0.025 mCi excreted in the first 8 min.

In all the subjects, urine obtained at the end of PET scanning was intensely radioactive. After correction for physical decay, 59%  $\pm$  7% of the injected radioactivity was present in the urine at 199  $\pm$  8 min (3.31 hr) after the injection.

Of the total urinary radioactivity, only 11% was due to unmetabolized [ $^{18}\text{F}$ ]-6F-DA. Since 59% of the injected radioactivity was present in urine at 3.31 hr after injection,  $0.11 \times 0.59 = 6\%$  of the injected [ $^{18}\text{F}$ ]-6F-DA was excreted unchanged.

After injection of [ $^{18}\text{F}$ ]-6F-DA, the concentration of radioactivity in whole blood declined in three phases (Tables 1 and 2). The plasma radioactivity concentration was less than that of whole blood during the first several minutes after administration of [ $^{18}\text{F}$ ]-6F-DA. Thereafter, the ratio of the radioactivity concentration in plasma to that in blood increased progressively, from a mean value less than 1 to a plateau mean value of 1.50 after about 10 min.

Assuming that the difference between the total plasma radioactivity concentration and the [ $^{18}\text{F}$ ]-6F-DA concentration reflected the concentration of metabolites of [ $^{18}\text{F}$ ]-6F-DA, the radioactive metabolites accumulated rapidly for several minutes after infusion and then declined slowly, approximately mono-exponentially, with a  $t_{1/2}$  of 84 min (1.39 hr biological disappearance constant,  $k = 0.495 \text{ h}^{-1}$ , Fig. 2).

## DISCUSSION

### Principles of [ $^{18}\text{F}$ ]-6F-DA Disposition

After injection of [ $^{18}\text{F}$ ]-6F-DA, the concentration of tissue radioactivity, and therefore organ visualization by PET scanning, depends on regional blood flow, transcapillary delivery of the drug to the interstitium, the density of sympathetic innervation, the avidity of neuronal and extra-neuronal removal processes, and the effectiveness of vesicular storage in local sympathetic nerves. Organs possessing intense sympathetic innervation include the heart, salivary glands, spleen, gut, kidneys and vascular smooth muscle; organs with relatively sparse innervation include

the skeletal muscle, skin, liver, pulmonary parenchyma and bone.

Sympathetically innervated organs store injected [ $^3\text{H}$ ]-6F-DA-derived radioactivity mainly as [ $^3\text{H}$ ]-6F-DA and [ $^3\text{H}$ ]-6F-NE (4). Turnover rates of these stored compounds eventually determine the rate of loss of radioactivity. This explains why the slopes of the time-activity curves for myocardium, liver, blood, plasma and metabolites of [ $^{18}\text{F}$ ]-6F-DA eventually became similar ( $k$  values of 0.444, 0.456, 0.475, 0.479 and  $0.497 \text{ h}^{-1}$ ) in this study.

Because of the effective blood-brain barrier for catecholamines (17), including [ $^{18}\text{F}$ ]-6F-DA (6), little if any of the radiolabeled compound enters the brain.

Since injected [ $^{18}\text{F}$ ]-6F-DA exits the circulation rapidly, and since both neuronal and non-neuronal cells remove and metabolize the drug, radiation doses to excretory organs—the kidneys, urinary bladder, liver and gallbladder—after [ $^{18}\text{F}$ ]-6F-DA administration depend on rates of excretion of the radioactive metabolites of [ $^{18}\text{F}$ ]-6F-DA. In this study, 59% of the injected radioactivity was present in the urine 3.31 hr after the injection of [ $^{18}\text{F}$ ]-6F-DA. Excretion of unmetabolized [ $^{18}\text{F}$ ]-6F-DA accounted for only 6% of the injected radioactivity.

The following discussion presents estimated radiation doses in descending order, beginning with the organs receiving the highest doses. For the heart, liver, gallbladder, lungs, bone and skeletal muscle, the estimates took into

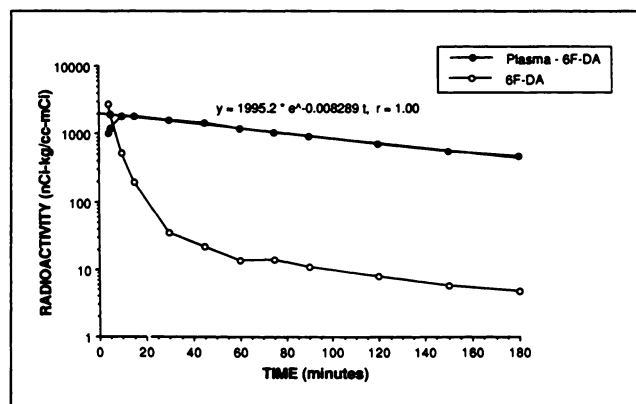


**FIGURE 2.** Mean arterial plasma concentrations of [ $^{18}\text{F}$ ]-6F-DA and the difference between plasma and [ $^{18}\text{F}$ ]-6F-DA concentrations after injection of [ $^{18}\text{F}$ ]-6F-DA into humans.

account actual radioassay results. For other organs, radioassay predictions depended on the radioactivity concentrations in the above organs and in blood and urine.

### Urinary Bladder Wall

The bases for the estimates of radiation exposure to the wall of the urinary bladder and to the kidneys were the data from the present study and a previously described model for the kinetics of [<sup>18</sup>F]-6F-DA-derived radioactivity in the plasma, renal pelvises, and urinary bladder (7). The model assumes that the [<sup>18</sup>F]-6F-DA is administered as a bolus at time  $t = 0$  min.

In this model,  $k_1$  is the estimated rate constant for the late phase of decline of the plasma level of radioactivity (after correction for decay). The value for  $k_1$  includes losses via the hepatobiliary as well as urinary systems; however, the present results indicate that virtually all the loss is via the urinary system. In this study,  $k_1$  was  $0.479 \text{ h}^{-1}$ .

$k_2$  is the estimated rate constant for loss of radioactivity from the collecting tubules and pelvises and is determined by the rate of urine flow divided by the volume of urine in the renal pelvises. The total effective volume of each renal pelvis was assumed to be 30 ml, or 60 ml for both kidneys. The value for  $k_2$  was calculated from the observed mean value for urine flow,  $72 \text{ ml} \cdot \text{h}^{-1}$  (excluding any brief diuresis) divided by the estimated effective renal pelvic volume;  $k_2$  therefore was  $1.20 \text{ h}^{-1}$ .

There were two components to the excretion of the radioactive compound during PET scanning: an initial "flush" of rapid excretion of [<sup>18</sup>F]-6F-DA-derived radioactivity,  $I_o$ , estimated to be 4% or less of the administered dose, and a slower component,  $P_o$ , derived from the portion of the remainder of the dose that was available for excretion and not sequestered in storage sites. Since there is substantial storage, the effective  $P_o$  value was less than the injected amount ( $A_o$ ).

The value of  $I_o$  was calculated as follows. In the subject with an indwelling Foley catheter, after administration of 2.0 mCi of [<sup>18</sup>F]-6F-DA, the total amount of radioactivity (corrected for decay) in urine during the first 3 hr was 0.481 mCi, and 0.025 mCi was excreted in the first 8 min.  $I_o$  was assumed to be delivered into the renal pelvis with a delay of 1 min; the urine flow rate during the initial "flush" was assumed to be that during the initial 8-min diuresis ( $370 \text{ ml} \cdot \text{h}^{-1}$ ); and the delivery of urine from the renal pelvis into the bladder was assumed to contribute another delay of 1 min.

The amount of radiolabeled compound in the bladder,  $B_1$ , at time  $t$  is:

$$B_1 = I_o[1 - e^{-k'_2(t - 2/60)}], \quad \text{Eq. 1}$$

where  $k'_2$  is the diuretic flow during the initial flush ( $370 \text{ ml} \cdot \text{h}^{-1}$ ), divided by the estimated effective renal pelvic volume (60 ml), or  $6.166 \text{ h}^{-1}$ . Ignoring the small contribution of  $P_o$  at this time, Equation 1 yields a value for  $I_o$  of  $0.027 A_o$ —i.e., 2.7% of the administered dose.

Given the above value for  $I_o$ , the value for  $P_o$  was calculated. By 3.31 hr after administration, a mean of 59.2% of the dose (corrected for decay) had been excreted. Since 2.7% of this was  $I_o$ , the remainder, 56.5%, was excreted after the initial flush.  $R_p$ , the amount of the labeled compound from  $P_o$ , corrected for decay, that is in compartment R (the renal pelvises) at time  $t$  is:

$$R_p = [(k_1 P_o)/(k_2 - k_1)](e^{-k_1 t} - e^{-k_2 t}), \quad \text{Eq. 2}$$

since

$$dB_p/dt = k_2 R_p. \quad \text{Eq. 3}$$

Substituting  $R_p$  from Equation 2 and solving for  $B_p$  gives the total compound from  $P_o$  (corrected for decay) excreted by 3.31 hr:

$$B_p = [k_1 k_2 P_o / (k_2 - k_1)] [(1 - e^{-k_1 t})/k_1 - (1 - e^{-k_2 t})/k_2] \\ = 0.672 P_o, \quad \text{Eq. 4}$$

since  $B_p = 0.565 A_o$  at 3.31 hr,  $0.565 A_o = 0.672 P_o$ , so  $P_o = 0.841 A_o$ .

These results indicate that during the 3-hr period of PET scanning after [<sup>18</sup>F]-6F-DA injection, about one-sixth of the [<sup>18</sup>F]-6F-DA-derived radioactivity was sequestered in a pool different from the plasma. Three findings are consistent with this inference. First, the fraction of the initial radioactive drug remaining in the tissues at 3.31 hr after injection of [<sup>18</sup>F]-6F-DA was estimated by applying the equation for the bi-exponential curve of best fit for the myocardial PET data:  $M_{3.31} = 4754 e^{-(2.80)(3.31)} + 4669 e^{-(0.444)(3.31)} = 1074 \text{ nCi} \cdot \text{kg}/\text{cc} \cdot \text{mCi}$ . This value corresponded to 17.8% of the myocardial radioactivity concentration observed in the first PET scanning interval. Second, assuming all the radioactive drug was present in cells, extracellular fluid (including plasma), and the urinary system (including the renal pelvises and bladder) at 3.31 hr after injection of [<sup>18</sup>F]-6F-DA, the proportion in cells could be estimated. At 3.31 hr, 59% of the injected drug was in bladder urine; application of Equation 2 yielded a value of 10% of the injected drug in the urinary system at 3.31 hr; and assuming rapid equilibration of radioactivity between the extracellular fluid and plasma, extracellular fluid volume of 27% of body weight (Ref. 17, 21,300 ml in the present study), and plasma radioactivity concentration of  $411.9 \text{ nCi} \cdot \text{kg}/\text{cc} \cdot \text{mCi}$  at 3.31 hr (from  $477.8 \text{ nCi} \cdot \text{kg}/\text{cc} \cdot \text{mCi}$  at 3.0 hr and application of the equation  $P_{3.31} = 477.8 e^{-(0.479)(0.31)}$ ), 11% of the injected drug was in the extracellular fluid at 3.31 hr. Therefore, about  $100 - 59 - 10 - 11 = 20\%$  of the injected drug was in cells at 3.31 hr. Third, from the equation for the line of best fit for the late component of the decline of plasma radioactivity,  $e^{-(0.479)(3.31)}$ , or 20%, of the  $P_o$  amount for this component was present in plasma at 3.31 hr after injection of [<sup>18</sup>F]-6F-DA. Since the rate constants for organ radioactivity and plasma radioactivity were similar by this time, one may infer that about 20% of the administered [<sup>18</sup>F]-6F-DA-derived radio-

activity remained in the organs at 3.31 hr and so had not entered the plasma.

To quantify the total radiation exposure to the wall of the urinary bladder, due to the radioactive urine contents, the contributions from the two components,  $P_o$  and  $I_o$ , were considered separately.  $A_{B_p}$ , the amount of radioactivity in the bladder from  $P_o$  at any time,  $t$ , is:

$$A_{B_p} = B_p e^{-k_D t} = [(k_1 k_2 P_o) / (k_2 - k_1)] \left[ \frac{(1 - e^{-k_1 t})}{k_1} - \frac{(1 - e^{-k_2 t})}{k_2} \right] \cdot e^{-k_D t}, \quad \text{Eq. 5}$$

where  $k_D$  is the physical decay constant,  $0.381 \text{ h}^{-1}$ . (For  $P_o$  the delay in transfer from plasma via the kidneys and ureters to the bladder can be ignored.) Integration of this activity over the time to voiding, 3.31 hr, obtains the cumulative activity,  $\bar{A}_{B_p}$ ,

$$\bar{A}_{B_p} = [(k_1 k_2 P_o) / (k_2 - k_1)] \left[ \frac{(1 - e^{-k_1 t})}{k_1 k_D} - \frac{(1 - e^{-(k_1 + k_D)t})}{k_1 (k_1 + k_D)} \right] - \left[ \frac{(1 - e^{-k_2 t})}{k_2 k_D} - \frac{(1 - e^{-(k_2 + k_D)t})}{k_2 (k_2 + k_D)} \right], \quad \text{Eq. 6}$$

or 1.61 mCi-h for a 4-mCi injection.

For calculating  $\bar{A}_{B_i}$ , the cumulative activity due to  $I_o$  by 3.31 hr, it was assumed that all the drug from the initial flush would be excreted in the urine by 3.31 hr; that is, from Equation 1,  $B_i = I_o = 0.027 A_o$ . The amount of radioactivity due to the drug from the initial flush is

$$A_{B_i} = 0.027 A_o e^{-k_D t}. \quad \text{Eq. 7}$$

Integrating from time  $t = 0$  to time  $t = 3.31$  hr, results in

$$\bar{A}_{B_i} = 0.027 A_o (1 - e^{-k_D t})$$

or 0.077 mCi-h for a 4-mCi injection. The total cumulative activity at 3.31 hr therefore would be  $1.61 + 0.08 = 1.70$  mCi-h for a 4-mCi injection.

The proportion of radioactivity remaining in the plasma at time  $t$  was  $e^{-(k_1 + k_D)t}$ . At 3.31 hr, this amount was 5.80% of  $P_o$ . During the next 3.31-hr interval, application of Equation 6, using this value for  $P_o$  yielded a cumulative activity of 0.093 mCi-h. Assuming the subject voided every 3.31 hr, repeated application of Equation 6, with progressively reduced values for  $P_o$ , led to a total amount of radioactivity exposure in the bladder, including that due to the initial flush, of 1.78 mCi-h after injection of 4 mCi of  $^{18}\text{F}$ -6F-DA. For an S-factor of 1.81 rad/mCi-h, the estimated absorbed dose to the bladder wall, due to the bladder contents, would be 3.22 rads.

### Kidneys

The kidneys remove in one circulation about 60% of the catecholamine content in the arterial plasma flowing to them (19), and the kidneys receive about 25% of the cardiac output (17). Thus, during the first circulation through the kidney, 15% of the arterial plasma catecholamine content would be removed, during the second (assuming 50% extraction of catecholamines by the body as a whole), an

additional 7.5% would be removed, and so forth, leading to an initial renal "load" of 29% of the injected dose. Since 2.7% of the injected drug was excreted during the "flush," 26.3% ( $= 29\% - 2.7\%$ ) of the injected dose was assumed to persist long enough in the kidneys to contribute to the renal absorbed radiation dose.

$\bar{A}_R$ , the cumulative radioactivity due to the radioactive urine contents of the renal pelvises, was calculated from:

$$\bar{A}_R = [k_1 / (k_2 - k_1)] \{ P_o [(1 / (k_1 + k_D)) - (1 / (k_2 + k_D))] + (I_o / (k_2 + k_D)) \}. \quad \text{Eq. 8}$$

For a 4-mCi injected dose, the radioactivity exposure to the kidneys due to the flush would be 0.02 mCi-hr and that after the flush would be 1.19 mCi-hr, for a cumulative radioactivity exposure of 1.20 mCi-hr. For an S-factor of 2.32 rad/ $\mu\text{Ci-hr}$ , the estimated absorbed dose to the kidneys, due to the radioactivity in the kidneys, would be 2.78 rads.

### Portal-Drained Viscera

About 20% of the cardiac output is distributed to the portal-drained viscera (17), and a reasonable estimate is that about 50% of circulating radiolabeled catecholamine is removed in the portal-drained viscera during a single circulation. Thus, in the first circulation, the amount of radioactivity retained in the viscera would be  $0.20 \times 0.50$  or 10% of the injected amount. Given 50% recirculation, a total of about 19% of the injected radioactivity would be taken up in the portal-drained viscera.

PET scanning did not depict these organs clearly, probably because of the large volumes and therefore low radioactivity concentrations of the organs (including the spleen, stomach and small intestine) draining into the portal vein.

Assuming a mono-exponential decline in the radioactivity concentration in the portal-drained viscera with time after injection of  $^{18}\text{F}$ -6F-DA, with a biological  $t_{1/2}$  of 1.5 hr, the integrated visceral radioactivity exposure,  $A_V$ , can be calculated. If  $A_V$  is the amount of radioactivity in the viscera at time,  $t$ , then

$$A_V = (\%V/100 \cdot A_o) \cdot e^{-k_V t} \cdot e^{-k_D t} = (\%V/100 \cdot A_o) \cdot e^{-(k_V + k_D)t}, \quad \text{Eq. 9}$$

where  $\%V/100$  is the proportion of the injected dose that is taken up in the viscera,  $A_o$  is the amount of the injected dose, and  $k_V$  is the biological  $k$  value. Integrating from  $t = 0$  to  $t = \infty$ ,

$$\bar{A}_V = (\%V/100 \cdot A_o) \cdot [1 / (k_V + k_D)], \quad \text{Eq. 10}$$

Since

$$t_{1/2 \text{ eff}} = (t_{1/2 \text{ biol}} \cdot t_{1/2 \text{ phys}}) / (t_{1/2 \text{ biol}} + t_{1/2 \text{ phys}}), \quad \text{Eq. 11}$$

where  $t_{1/2 \text{ biol}}$  is the biological half-time and  $t_{1/2 \text{ phys}}$  is the physical half-time, and since

$$k_{\text{eff}} = k_V + k_D,$$

where  $k_{\text{eff}}$  is the effective  $k$  value,

$$\bar{A}_V = 1.44(\%V/100 \cdot A_0) \cdot t_{1/2 \text{ eff}} \quad \text{Eq. 12}$$

In the portal-drained viscera,  $t_{1/2 \text{ eff}} = 0.82$  hr, and for a 4-mCi dose,  $\bar{A}_V = 0.90$  mCi-h.

In the liver and heart, however, the declines in [ $^{18}\text{F}$ ]-6F-DA-derived radioactivity were bi-exponential. Values for integrated radioactivity exposure to the portal-drained viscera therefore were estimated from the expected  $t_{1/2}$  and y-intercept values for the early and late phases, considered separately and then summed. Given the similar y-intercept values for the early and late phases in the heart and liver, the proportion of the injected dose constituting the "load" to the portal-drained viscera during the early and late phases,  $F_{V \text{ early}}$  and  $F_{V \text{ late}}$ , may be assumed to be about 50% of the total "load", or 9.5% of the injected dose. If the early and late  $t_{1/2 \text{ biol}}$  values were 0.25 and 1.50 hr, then the early and late  $t_{1/2 \text{ eff}}$  values would be 0.22 and 0.82 hr. Thus, for the early phase,

$$\begin{aligned} \bar{A}_{V \text{ early}} &= 1.44(\%V/100 \cdot F_{V \text{ early}} \cdot A_0) \cdot (t_{1/2 \text{ eff early}}) \\ &= 0.03 \text{ mCi-h per mCi injected,} \quad \text{Eq. 13} \end{aligned}$$

and for the late phase,

$$\begin{aligned} \bar{A}_{V \text{ late}} &= 1.44(\%V/100 \cdot F_{V \text{ late}} \cdot A_0) \cdot (t_{1/2 \text{ eff late}}) \\ &= 0.11 \text{ mCi-h per mCi injected,} \quad \text{Eq. 14} \end{aligned}$$

From

$$\bar{A}_{V \text{ total}} = \bar{A}_{V \text{ early}} + \bar{A}_{V \text{ late}} \quad \text{Eq. 15}$$

$\bar{A}_{V \text{ total}}$  is 0.14 mCi-h for a 1-mCi dose, or 0.57 mCi-h for a 4-mCi dose.

Assuming the small intestine, spleen and stomach constitute 3/5, 1/5 and 1/5 of the portal-drained viscera, then the  $\bar{A}_V$  total values for the small intestine, spleen and stomach would be 0.34, 0.11 and 0.11 mCi-h for a 4-mCi dose.

#### Liver

Tissue radioactivity in the liver declined bi-exponentially. The estimated initial radioactivity concentration was the sum of the y-intercept values for the early and late phases,  $4398 + 4802 = 9200$  nCi-kg/cc-mCi. For a 4 mCi dose of [ $^{18}\text{F}$ ]-6F-DA in a 70-kg subject with hepatic volume of 1000 cc, this would represent 526  $\mu\text{Ci}$ , or 13% of the administered dose. From the bi-exponential curve of best fit for the relationship between hepatic radioactivity and time, calculated  $t_{1/2 \text{ eff}}$  values were 0.29 and 0.61 hr for the two phases. Applying Equations 10 through 15 yields  $\bar{A}_L$  values of 0.10 and 0.24 mCi-h for each phase, with a total  $\bar{A}_L$  value of 0.34 mCi-h for a 4-mCi injection.

#### Myocardium

The decline in myocardial radioactivity was also bi-exponential. From the y-intercept values for the early and late phases, the initial ( $t = 0$ ) calculated initial radioactivity concentration was  $4754 + 4669 = 9423$  nCi-kg/cc-mCi. For a 4-mCi dose in a 70-kg subject with a myocardial volume of 300 cc, this would represent 162  $\mu\text{Ci}$ , or 4% of the

administered dose. Since only about 5% of the cardiac output is distributed to the myocardium (17), the results confirm that the myocardium avidly removes [ $^{18}\text{F}$ ]-6F-DA-derived radioactivity.

From the bi-exponential curves of best fit, calculated values for  $t_{1/2 \text{ eff}}$  values were 0.22 and 0.84 hr. Applying Equations 10 through 15, the  $\bar{A}_M$  values were 0.00 and 0.10 for each phase, with a total  $\bar{A}_M$  value of 0.10 mCi-h for a 4-mCi injection.

#### Skeletal Muscle and Skin

Although the uptake of [ $^{18}\text{F}$ ]-6F-DA-derived radioactivity in the limbs would be expected to be substantial (15% of the injected amount), the radioactivity would be expected to decline rapidly in a manner similar to the plasma radioactivity, because only about 15% of catecholamine in the arterial inflow is removed by neuronal uptake (10). The rapid early loss of radioactive O-methylated metabolites would decrease the organ radioactivity exposure. After a few minutes, radioactivity in the limbs would be due to uptake and storage in the regional sympathetic nerves.

For purposes of estimating absorbed doses, the initial load of [ $^{18}\text{F}$ ]-6F-DA-derived radioactivity in skeletal muscle was assumed to correspond to the neuronal uptake by the limbs—about  $0.15 \times 0.15$  or 2.3% of the injected amount. If the  $t_{1/2 \text{ biol}}$  value were 1.5 hr, similar to the value in the myocardium, then the  $t_{1/2 \text{ eff}}$  value would be 0.82 hr, and application of Equation 12 would yield an integrated radioactivity exposure of 0.11 mCi-h for a 4-mCi dose.

#### Gallbladder

At the end of PET scanning, the concentration of [ $^{18}\text{F}$ ]-6F-DA-derived radioactivity,  $G_{SS}$ , was about 11,000 nCi-kg/cc-mCi (decay-corrected). For a gallbladder volume of 30 cc, subject mass of 70 kg and dose of 4 mCi, this would correspond to  $11,000 \times 30 \times 4/70/1000 = 19 \mu\text{Ci}$ , or about 0.5% of the administered dose. This contrasts with the over 100-fold greater amount of the administered dose that was excreted in the urine. Thus, virtually all injected [ $^{18}\text{F}$ ]-6F-DA-derived radioactivity is excreted in the urine.

If the only source of radioactivity in the bile was from hepatic excretion, and assuming no gallbladder emptying during the PET scanning, the amount of drug in the bile at time  $t$ ,  $G_t$ , would be related to the rate constant for transfer from the liver to the gallbladder,  $k_{LG}$ , by the equation,

$$G_t = G_{SS} \cdot (1 - e^{-k_{LG}t}). \quad \text{Eq. 16}$$

The amount of radioactivity in the gallbladder at time  $t$ ,  $A_G$ , is:

$$A_G = G_t e^{-k_D t} = G_{SS} \cdot (e^{-k_D t} - e^{-(k_{LG} + k_D)t}). \quad \text{Eq. 17}$$

The integrated radioactivity in the gallbladder,  $\bar{A}_G$ , is then:

$$\begin{aligned} \bar{A}_G &= G_{SS} \cdot [((1 - e^{-k_D t})/k_D) \\ &\quad - (1 - e^{-(k_D + k_{LG})t})/(k_D + k_{LG})]. \quad \text{Eq. 18} \end{aligned}$$

A conservative estimate for the  $t_{1/2}$  for the transfer from liver to gallbladder is 1.5 hr, for an estimated  $k_{LG}$  value of

0.462 h<sup>-1</sup>. Applying this value in Equation 18, and assuming a gallbladder volume of 30 cc and subject weight of 70 kg,  $\bar{A}_G$  is 0.015 mCi-h for a 4-mCi dose.

### Brain, Lungs and Bone

After injection of [<sup>18</sup>F]-6F-DA into dogs, little if any [<sup>18</sup>F]-6F-DA-derived radioactivity is detected in brain, demonstrating the effective blood-brain barrier for catecholamines (20). Therefore, the radioactivity exposure to the brain due to tissue uptake of [<sup>18</sup>F]-6F-DA would be small and would depend mainly on tissue radioactivity due to retention of radioactive circulating metabolites of [<sup>18</sup>F]-6F-DA and from radioactivity in the blood perfusing the brain (Table 3).

Analogously, since little or no [<sup>18</sup>F]-6F-DA-derived radioactivity accumulated in regions corresponding to pulmonary parenchyma and the spine, one may infer that radiation doses to the lungs, bony surfaces and red marrow would also be small. Because of the low pulmonary extraction fraction of [<sup>3</sup>H]-NE (11), most of the radioactivity exposure to the lungs would probably result from retention of radioactive metabolites of [<sup>18</sup>F]-6F-DA and from radioactivity in the blood perfusing the lungs.

### Noninnervated, Nonexcretory Organs

The present results enabled estimation of the integrated radioactivity exposure due to the radioactivity in metabolites of [<sup>18</sup>F]-6F-DA in plasma and due to the radioactivity in whole blood.

*Tissue Radioactivity Due to Partial Retention of Radioactive Metabolites.* Even in the absence of cellular uptake of [<sup>18</sup>F]-6F-DA, organs would still undergo radiation exposure due to the persistence of metabolites of the radiochemical in the plasma, since the radioactive metabolites in plasma could equilibrate with the intracellular space. For noninnervated or sparsely innervated organs, radioactivity doses due to intracellular metabolites of [<sup>18</sup>F]-6F-DA would be expected to be small but can be estimated. The difference between the total plasma radioactivity concentration and the plasma [<sup>18</sup>F]-6F-DA concentration was assumed to reflect the concentration of metabolites of [<sup>18</sup>F]-6F-DA. In a noninnervated organ,  $N_p$ , the concentration of radioactivity in the cells, would be due almost entirely to radioactive metabolites of [<sup>18</sup>F]-6F-DA.  $N_p$  was estimated as 0.17 times the plasma radioactive metabolite concentration (7). From the mono-exponential line of best fit for the decline in the plasma radioactive metabolite concentration with time, the  $y_0$  value for the radioactive metabolite concentration,  $y_{0-\text{metab}}$ , is 1995 nCi-kg/cc-mCi, and the  $k$  value,  $k_{\text{metab}}$ , is 0.50 h<sup>-1</sup>. The amount of radioactivity in the organ,  $A_N$ , at time,  $t$ , is:

$$A_N = 0.17 y_{0-\text{metab}} e^{-(k_{\text{metab}} + k_D)t} \quad \text{Eq. 19}$$

Integration of  $A_N$  yields

$$\begin{aligned} \bar{A}_N &= 0.17 y_{0-\text{metab}} / (k_{\text{metab}} + k_D) \\ &= 385 \text{ nCi-kg-hr/cc-mCi.} \quad \text{Eq. 20} \end{aligned}$$

In the lungs, for a volume of 6,000 cc in a 70-kg subject,  $\bar{A}_N$  would be 0.13 mCi-h for a 4-mCi dose. In the brain (assuming a brain volume of 1,500 cc and a completely ineffective blood-brain barrier for radioactive metabolites of [<sup>18</sup>F]-6F-DA),  $\bar{A}_N$  would be 0.03 mCi-h for a 4-mCi dose.

*Tissue Radioactivity Due to Blood Radioactivity.* The radioactivity in blood may be considered to be a source of exposure to all perfused organs. The amount of radioactivity in a target organ at any time, due to the radioactivity in blood, would be the blood radioactivity concentration times the volume of blood in the organ. Since a tri-exponential curve was required to fit the blood radioactivity data in Figure 1, the amount of radioactivity in the arterial blood,  $A_B$ , at time,  $t$ , is

$$A_B = A_{B1} + A_{B2} + A_{B3}, \quad \text{Eq. 21}$$

where  $A_{B1}$ ,  $A_{B2}$  and  $A_{B3}$  are the amounts of radioactivity for each of the three phases. For each phase,  $X$ ,

$$A_{BX} = A_{BX0} e^{-(k_{\text{ax}} + k_D)t}, \quad \text{Eq. 22}$$

where  $A_{BX0}$  is the y-intercept value for that phase and  $k_{BX}$  is the  $k$  value for that phase; and for each phase, the cumulative radioactivity,  $\bar{A}_{BX}$  is:

$$\bar{A}_{BX} = A_{BX0} / (k_{BX} + k_D). \quad \text{Eq. 23}$$

The total cumulative blood radioactivity is

$$\begin{aligned} \bar{A}_B &= A_{B10} / (k_{B1} + k_D) + A_{B20} / (k_{B2} \\ &+ k_D) + A_{B30} / (k_{B3} + k_D). \quad \text{Eq. 24} \end{aligned}$$

During the early, middle and late phases, the  $k$  values for blood radioactivity were 29.1, 5.93 and 0.475 h<sup>-1</sup> and the y-intercept values 21,921, 1,921 and 1,249 nCi-kg/cc-mCi for the three phases. Applying these values in Equation 24, the total radioactivity exposure to noninnervated organs, due to the blood radioactivity, would be 744 + 304 + 1459 = 2507 nCi-kg-hr/cc-mCi, or 0.00251 mCi-kg-hr/cc-mCi. For the lungs, with 520 cc of blood (21), radioactivity exposure due to blood radioactivity after a 4-mCi dose of [<sup>18</sup>F]-6F-DA into a 70-kg person would be 0.075 mCi-h; and for the brain, with 260 cc of blood (21), the radioactivity exposure due to blood radioactivity would be 0.037 mCi-h.

Thus, the total radioactivity exposure to the lungs, from intracellular radioactive metabolites and from radioactivity in blood, would be 0.13 + 0.08 = 0.21 mCi-h for a 4-mCi injection. Analogously, the total radioactivity exposure to the brain from these sources would be 0.07 mCi-h.

### Absorbed Dose Estimates

Estimates of absorbed doses using the MIRDOSE program depend on values for "mean retention time,"  $\tau$ . These values can be calculated in two ways. One is from the ratio of the integrated radioactivity exposure-to-the amount injected:

$$\tau = \bar{A} / A_0. \quad \text{Eq. 25}$$



**TABLE 3**  
Values for Pharmacokinetic Parameters After Injection of 6-[<sup>18</sup>F]Fluorodopamine

Organ	[ <sup>18</sup> F]Fluorodopamine Percent Load	$\bar{A}$ (mCi-h)
Urinary bladder contents	2.7	1.78
Kidneys	26.3	1.20
Liver	13.0	0.34
Small intestine	0.0	0.34
Lungs	11.4	0.21
Spleen	3.8	0.11
Stomach	3.8	0.11
Skeletal muscle	2.3	0.11
Myocardium	4.0	0.10
Brain	0.5	0.07
Gallbladder contents	0.0	0.02
Other	32.2	
Total	100.0	

The second applies Equations 12 and 25, yielding the formula  $\tau = 1.44 (\%V/100) t_{1/2 \text{ eff}}$ . For the source organ, "total body," only the latter approach was feasible, since  $\bar{A}$  values for this source were not obtained. After injection of [<sup>18</sup>F]-6F-DA,  $t_{1/2 \text{ bio}}$  could be assumed to be 1.4 hr, corresponding to the late  $t_{1/2}$  for the decline of plasma radioactivity. This would yield a  $t_{1/2 \text{ eff}}$  value of 0.79 hr and  $\tau$  0.37 hr for "total body."

This approach using the MIRDOSE program does not appear to take into account the multi-exponentiality of declines in tissue radioactivity after [<sup>18</sup>F]-6F-DA administration. The estimated absorbed doses listed in Table 4 therefore were calculated using a computer spreadsheet, with the total absorbed dose in a given target organ being the sum of values for  $\bar{A} \cdot S$  for each source organ.

The present analysis assumes a constant volume bladder. A higher urine volume at the time of injection and enlargement of the bladder during the PET scanning would be expected to decrease the absorbed radiation dose for a given amount of cumulative activity (22).

#### Estimates of Organ Radiation Doses After Injection of [<sup>3</sup>H]-L-Norepinephrine

As noted above, the fate of injected [<sup>18</sup>F]-6F-DA generally resembles that of other radiolabeled catecholamines. The measurements of organ radioactivity concentrations by PET scanning and of blood, plasma and urine concentrations of [<sup>18</sup>F]-6F-DA and its metabolites provided a basis for estimating organ radiation doses after injection of [<sup>3</sup>H]-1-NE, a radiolabeled drug used to assess the rate of appearance of endogenous NE in plasma (NE spillover) in humans (10-12).

For these estimates, integrated radioactivity exposures due to the radioactivity in metabolites of [<sup>3</sup>H]-NE in plasma and due to the radioactivity in whole blood were assumed to be negligibly small.

Clinical studies of [<sup>3</sup>H]-L-NE kinetics have often used a constant infusion technique, with doses of about 0.75-1.5  $\mu\text{Ci}$ , or a total dose of about 100  $\mu\text{Ci}$ , corresponding to about 2.5% of the dose of [<sup>18</sup>F]-6F-DA used for PET scanning. The much smaller dose of radioactive drug, and the fact that S-factors for converting integrated radioactivity exposure to absorbed radiation doses are much smaller for [<sup>3</sup>H]-labeled compounds than for [<sup>18</sup>F]-labeled compounds, led to very small estimated radiation doses ( $\leq 0.003$  rem for all organs) after [<sup>3</sup>H]-L-NE administration (Table 5), compared with estimated doses after [<sup>18</sup>F]-6F-DA administration.

**TABLE 4**  
Estimates of Absorbed Radiation Doses to Body Organs After Intravenous Injection of 4 mCi of 6-[<sup>18</sup>F]Fluorodopamine in Humans

Target Organ	Dose (rem)	Primary source (Organ, rem)	Secondary source (Organ, rem)
Urinary bladder wall	3.27	Bladder contents, 3.22	Total body, 0.03
Kidneys	2.85	Kidneys, 2.78	Total body, 0.03
Spleen	0.55	Spleen, 0.43	Kidneys, 0.07
Uterus	0.36	Bladder contents, 0.20	Small intestine, 0.03
Small intestine	0.36	Small intestine, 0.26	Bladder contents, 0.03
Heart wall	0.28	Heart wall, 0.21	Total body, 0.03
Gallbladder wall	0.25	Gallbladder contents, 0.12	Kidneys, 0.05
Stomach	0.25	Stomach, 0.15	Kidneys, 0.03
Liver	0.24	Liver, 0.16	Kidneys, 0.03
Lungs	0.18	Lungs, 0.13	Total body, 0.03
Ovaries	0.17	Bladder contents, 0.09	Small intestine, 0.03
Lower large intestine	0.17	Bladder contents, 0.09	Total body, 0.03
Adrenals	0.15	Kidneys, 0.09	Total body, 0.03
Pancreas	0.15	Kidneys, 0.06	Total body, 0.03
Upper large intestine	0.15	Small intestine, 0.05	Bladder contents, 0.03
Total body	0.10	Total body, 0.03	Kidneys, 0.02

Note: Doses  $\leq 0.10$  rem for all other target organs.

**TABLE 5**  
Estimates of Absorbed Radiation Doses to Body Organs After Intravenous Injection of 0.10 mCi of [<sup>3</sup>H]-L-Norepinephrine in Humans

Target Organ	Dose (rem)	Primary source (Organ, rem)	Secondary source (Organ, rem)
Urinary bladder wall	0.003	Bladder contents, 0.003	Total body, 0.000
Kidneys	0.003	Kidneys, 0.003	Total body, 0.000
All other organs	≤0.001		

## CONCLUSIONS

After intravenous injection of [<sup>18</sup>F]-6F-DA at a dose (4 mCi) adequate to visualize organ sympathetic innervation by PET scanning, about 60% of the injected radioactivity is excreted in the first void after a 3-hr interval. The organ receiving the highest radiation dose is the wall of the urinary bladder (about 3.3 rem, depending on the frequency of voiding after the PET scanning), with the kidneys receiving the next highest dose (2.9 rem) and with much smaller doses to all other organs. The estimated radiation dose to the wall of the urinary bladder in humans is about one-fourth that predicted from studies of anesthetized dogs (6). Urinary excretion of [<sup>18</sup>F]-6F-DA-derived radioactivity exceeds by over 100-fold hepatobiliary excretion of [<sup>18</sup>F]-6F-DA-derived radioactivity. Radiation doses to the brain are very small because of the effective blood-brain barrier for catecholamines. In noninnervated organs and the brain, small amounts of radiation exposure result from intracellular retention of metabolites of [<sup>18</sup>F]-6F-DA and from perfusion of the organs with radioactive blood.

Compared with organ radiation doses after administration of 4 mCi of [<sup>18</sup>F]-6F-DA into humans, radiation doses to all organs after administration of 100 μCi of [<sup>3</sup>H]-L-NE are negligibly small. Thus, co-administration of both radiolabeled compounds should yield virtually identical organ radioactivity exposures as administration of [<sup>18</sup>F]-6F-DA alone.

## ACKNOWLEDGMENTS

The authors thank Drs. Peter Herscovitch and Stephen Bacharach for helpful discussions to derive and present the formulas used in this manuscript and Courtney Holmes, CMT, for technical assistance.

## REFERENCES

- Chiueh CC, Zukowska-Grojec Z, Kirk KL, Kopin IJ. 6-F-fluorocatecholamines as false adrenergic neurotransmitters. *J Pharmacol Exp Ther* 1983; 225:529-533.
- Eisenhofer G, Hovey-Sion D, Kopin IJ, et al. Neuronal uptake and metabolism of 2- and 6-fluorodopamine: false neurotransmitters for positron emission tomographic imaging of sympathetically innervated tissues. *J Pharmacol Exp Ther* 1989;248:419-427.
- Hovey-Sion D, Eisenhofer G, Kopin IJ, et al. Metabolic fate of injected [<sup>3</sup>H]-dopamine and [<sup>3</sup>H]-2-fluorodopamine in rats. *Neuropharmacology* 1990;29:881-887.
- Chang PC, Szemerédi K, Grossman E, Kopin IJ, Goldstein DS. The fate of tritiated 6-fluorodopamine in rats: a false neurotransmitter for positron

emission tomographic imaging of sympathetic innervation and function. *J Pharmacol Exp Ther* 1990;255:809-817.

- Goldstein DS, Grossman E, Tamrat M, et al. Positron emission imaging of cardiac sympathetic innervation and function using [<sup>18</sup>F]-fluorodopamine: effects of chemical sympathectomy by 6-hydroxydopamine. *J Hypertens* 1991;9:417-423.
- Goldstein DS, Chang PC, Eisenhofer G, et al. Positron emission tomographic imaging of cardiac sympathetic innervation and function. *Circulation* 1990;81:1606-1621.
- Goldstein DS, Eisenhofer G, Dunn BB, et al. Positron emission tomographic imaging of cardiac sympathetic innervation using 6-[<sup>18</sup>F]-fluorodopamine: initial findings in humans. *J Am Coll Cardiol* 1993;22:1961-1971.
- Goldstein DS, Chang PC, Smith CB, et al. Dosimetric estimates for clinical positron emission tomographic scanning after injection of [<sup>18</sup>F]-6-fluorodopamine. *J Nucl Med* 1991;32:102-110.
- Ding YS, Fowler JS, Dewey SL, et al. Comparison of high specific activity (-) and (+)-6-[<sup>18</sup>F]-fluoronorepinephrine and 6-[<sup>18</sup>F]-fluorodopamine in baboons: heart uptake, metabolism and the effect of desipramine. *J Nucl Med* 1993;34:619-629.
- Goldstein DS, Zimlichman R, Stull R, et al. Measurement of regional neuronal removal of norepinephrine in man. *J Clin Invest* 1985;76:15-21.
- Goldstein DS, Cannon RO III, Quyyumi A, et al. Regional extraction of circulating norepinephrine, dopa, and dihydroxyphenylglycol in humans. *J Auton Nerv Sys* 1991;34:17-36.
- Eisenhofer G, Esler MD, Meredith IT, et al. Sympathetic nervous function in the human heart as assessed by cardiac spillovers of dihydroxyphenylglycol and norepinephrine. *Circulation* 1992;85:1775-1785.
- Dunn BB, Channing MA, Adams HR, Goldstein DS, Kirk KL, Kiesewetter DO. A single column, rapid quality control procedure for 6-[<sup>18</sup>F]-fluoro-L-dopa and 6-[<sup>18</sup>F]-fluorodopamine PET imaging agents. *J Nucl Med Biol* 1991;18:209-213.
- Eisenhofer G, Goldstein DS, Stull R, et al. Simultaneous liquid chromatographic determination of 3,4-dihydroxy-phenylglycol, catecholamines, and 3,4-dihydroxyphenylalanine in plasma, and their responses to inhibition of monoamine oxidase. *Clin Chem* 1986;32:2030-2033.
- Eisenhofer G, Kirk KL, Kopin IJ, Goldstein DS. Simultaneous determination of endogenous catechols and exogenous 2- and 6-fluorinated catechols in tissue and plasma using liquid chromatography with electrochemical detection. *J Chromatog* 1988;431:156-162.
- Loevinger R, Budinger TF, Watson EE. *MIRD primer for absorbed dose calculations*. New York: The Society of Nuclear Medicine; 1988.
- Shargel L, Yu ABC. *Applied biopharmaceutics and pharmacokinetics*. Norwalk, CN: Appleton-Century-Crofts; 1985.
- Snyder WS, Ford MR, Warner GG. Estimates of specific absorbed fractions for photon sources uniformly distributed in various organs of a heterogeneous phantom. *MIRD pamphlet no. 5, revised*. New York: Society of Nuclear Medicine, 1978.
- Zimlichman R, Goldstein DS, Eisenhofer G, Stull R, Keiser HR. Comparison of norepinephrine and isoproterenol removal in the canine hindlimb and kidney. *Clin Exp Pharmacol Physiol* 1986;13:777-781.
- Weil-Malherbe H, Axelrod J, Tomchick R. Blood-brain barrier for adrenaline. *Science* 1959;129:1226-1227.
- Poston JW, Aissi A, Hui TY, Jimba BM. A preliminary model of the circulating blood for use in radiation dose calculations. In: Schlafke-Stelson AT, Watson EE, eds. *Fourth international radiopharmaceutical dosimetry symposium*. Oak Ridge, TN: Oak Ridge Associated Universities; 1986:574-586.
- Thomas SR, Stabin MG, Chen C-T, Samaratinga RC. MIRD pamphlet no. 14: a dynamic urinary bladder model for radiation dose calculations. *J Nucl Med* 1992;33:783-802.